Influence of meteorological variability on interannual variations of springtime boundary layer ozone over Japan during 1981–2005

J. Kurokawa[1], T. Ohara[1], I. Uno[2], M. Hayasaki[3], and H. Tanimoto[1]

[1]{National Institute for Environmental Studies, Onogawa, Tsukuba, Ibaraki, Japan}

[2]{Research Institute for Applied Mechanics, Kyushu University, Kasuga, Fukuoka, Japan}

[3]{Center for Environmental Remote Sensing, Chiba University, Yayoi, Inage, Chiba, Japan}

Correspondence to J. Kurokawa (kurokawa.junichi@nies.go.jp)

Supplementary Material

Relationships between springtime BL O_3 over western and central Japan and chemical processes

In order to evaluate the influence of chemical processes on the IAV of O_3 over WCJ, we examined the chemical production ($P(O_3)$), chemical loss ($L(O_3)$), and net chemical production ($N(O_3)$) of springtime BL O_3 simulated by $E_{00}M_{yy}$. $P(O_3)$, $L(O_3)$, and $N(O_3)$ are defined as follows:

$$P(O_3) = (k_4[HO_2] + k_5[CH_3O_2] + k_6[RO_2])[NO] \quad \text{(S1)}$$

$$L(O_3) = (k_1k_2[H_2O]/k_3[M] + k_7[OH] + k_8[HO_2])[O_3]$$

$$+ k_9[NO][O_3](k_{11}[NO_2][OH][M]/(k_{10}[NO_2] + k_{11}[NO_2][OH][M])) \quad (S2)$$

$$N(O_3) = P(O_3) – L(O_3) \quad (S3)$$

where k_i is the reaction rate coefficient for reaction K_i, listed in Table S1 and M denotes N_2 and O_2. By running CMAQ, $P(O_3)$, $L(O_3)$, and $N(O_3)$ were obtained every hour; then their springtime BL averages were calculated over East Asia during 1981–2005.

Figure S1 shows the composite anomaly fields of springtime BL $P(O_3)$ (a and b), $L(O_3)$ (c and d), and $N(O_3)$ (e and f) for high (a, c, and e) and low (b, d, and f) O_3 over WCJ years. During high O_3 over WCJ years, positive anomalies of $P(O_3)$ were found around the Yangtze Delta and western Japan. On the other hand, large positive anomalies of $L(O_3)$ (i.e., larger chemical destruction compared to the average) were widespread from the eastern coast of China to south of Japan. This area is almost the same as the region showing positive O_3 anomalies during high O_3 over WCJ years (Fig. 6c). As a result, there were positive anomalies of $N(O_3)$ over the southern part of WCJ and negative anomalies over the northern part. Relatively large positive $N(O_3)$ anomalies appeared over the eastern part of CEC, but elsewhere anomalies were small or, over the northern part of CEC, negative. Over the Korean peninsula, anomalies were negative during high O_3 over WCJ years. On the other hand, during low O_3 over WCJ years, anomalies of $P(O_3)$, $L(O_3)$, and $N(O_3)$ showed a very similar horizontal distribution to those during high O_3 over WCJ years but with opposite direction. $N(O_3)$ anomalies around WCJ were positive in the north and negative in the south. Anomalies of $N(O_3)$ showed large negative values over the eastern part of CEC, but elsewhere $N(O_3)$ anomalies showed small negative or positive values. Although clear differences in chemical processes over

East Asia are apparent between high and low O_3 over WCJ years, the effects of these processes on the IAV of O_3 are not obvious. Figure S2 displays scatter plots and regression lines (a) between anomalies of springtime BL O_3 and $N(O_3)$ over WCJ and (b) between anomalies of springtime BL O_3 over WCJ and $N(O_3)$ over CEC. Anomalies of O_3 and $N(O_3)$ over WCJ are clearly not related. On the other hand, anomalies of $N(O_3)$ over CEC are positively correlated with those of O_3 over WCJ. However, the slope of regression line is not large and the correlation coefficient is relatively small (0.37). These results suggest that the impact of chemical processes over East Asia on the IAV of O_3 over WCJ is small.

Table S1. Reactions in O_3 photochemistry used to calculate $P(O_3)$, $L(O_3)$, and $N(O_3)$.

K_1)	$O_3 + h\nu \rightarrow O_2 + O(^1D)$
K_2)	$O(^1D) + H_2O \rightarrow 2OH$
K_3)	$O(^1D) + M \rightarrow O(^3P) + M$
K_4)	$HO_2 + NO \rightarrow NO_2 + OH$
K_5)	$CH_3O_2 + NO \rightarrow NO_2 + CH_3O$
K_6)	$RO_2 + NO \rightarrow NO_2 + RO$
K_7)	$O_3 + OH \rightarrow HO_2 + O_2$
K_8)	$O_3 + HO_2 \rightarrow 2O_2 + OH$
K_9)	$NO + O_3 \rightarrow NO_2 + O_2$
K_{10})	$NO_2 + h\nu \rightarrow NO + O$
K_{11})	$NO_2 + OH + M \rightarrow HNO_3 + M$

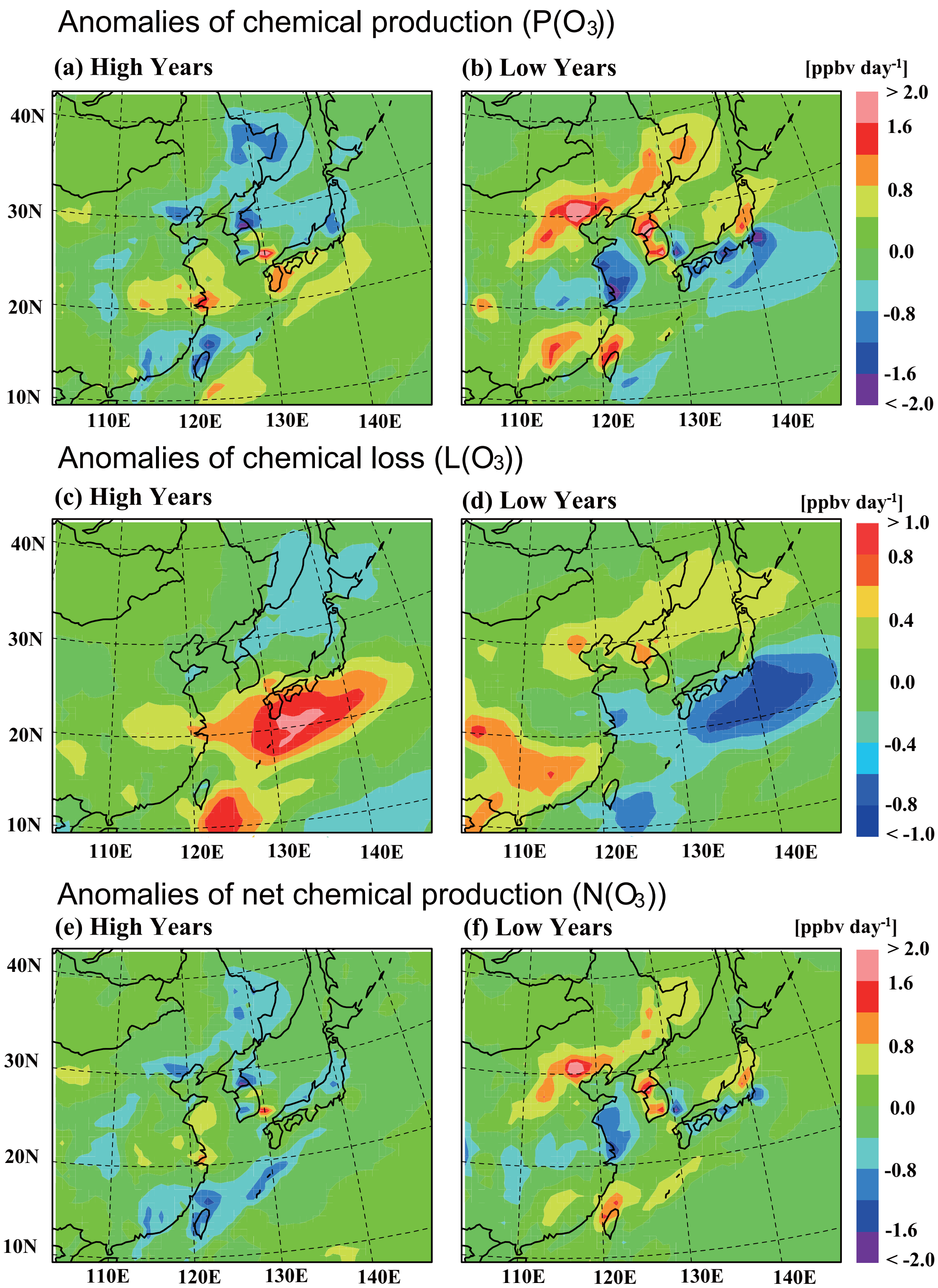
Anomalies of chemical production (P(O3))
(a) High Years
(b) Low Years
[ppbv day-1]
> 2.0
1.6
0.8
0.0
-0.8
-1.6
< -2.0
40N
30N
20N
10N
110E
120E
130E
140E
Anomalies of chemical loss (L(O3))
(c) High Years
(d) Low Years
[ppbv day-1]
> 1.0
0.8
0.4
0.0
-0.4
-0.8
< -1.0
Anomalies of net chemical production (N(O3))
(e) High Years
(f) Low Years
[ppbv day-1]
> 2.0
1.6
0.8
0.0
-0.8
-1.6
< -2.0

Figure S1. Composite spatial distributions of the anomalies of (a) chemical production ($P(O_3)$), (c) chemical loss ($L(O_3)$), and (e) net chemical production ($N(O_3)$) during high O_3 over WCJ years (High Years). The same information but during low O_3 over WCJ years (Low Years) is shown in (b), (d), and (f), respectively. High (low) O_3 over WCJ years were defined as the top (bottom) 5 years among the springtime BL O_3 anomalies over WCJ between 1981 and 2005. The $E_{00}M_{yy}$ scenario was used for the model simulation. Anomalies are defined as deviations from the averaged values during 1981–2005.

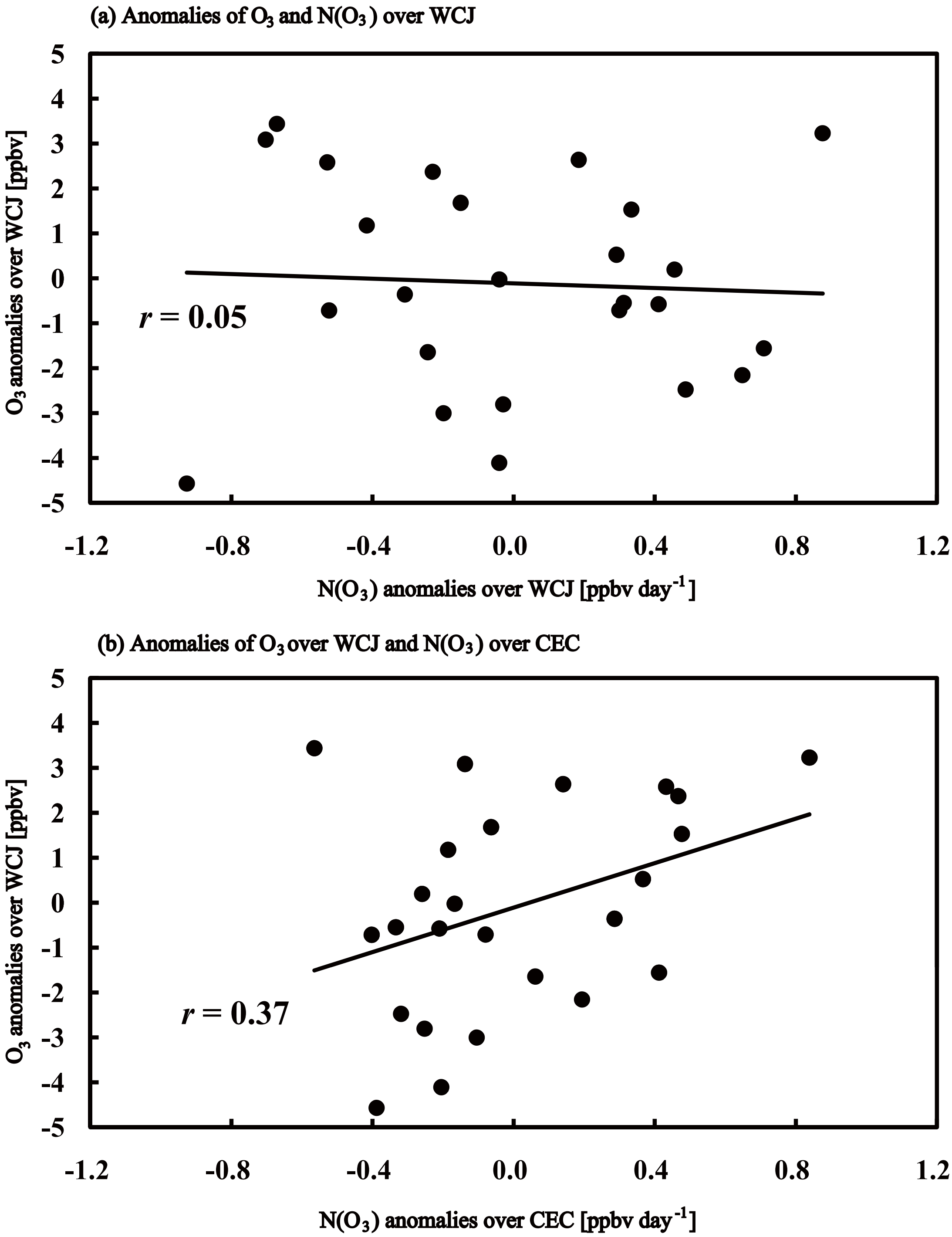

Figure S2. (a) Scatter plot and regression line between anomalies of springtime BL O_3 and $N(O_3)$ over WCJ during 1981–2005. (b) The same as in (a) but between anomalies of springtime BL O_3 over WCJ and $N(O_3)$ over CEC. The simulation scenario and the definition of anomalies are the same as in Fig. S1.